H2020 OPTICON project overview: investigating the use of additive manufacturing for the design and build of multi-functional integrated astronomical components

Hermine Schnetler, Bart van de Vorst, Robert M. Snell, Carolyn Atkins, Chris Miller, Katherine Morris, Szigfrid Farkas, György Mező, Mélanie Roulet, Emmanuel Hugot, Afrodisio Vega Moreno, Fabio Tenegi and Joris Dufils

Published version information:

Citation: H Schnetler et al. 'H2020 OPTICON project overview: investigating the use of additive manufacturing for the design and build of multi-functional integrated astronomical components.' Proceedings of SPIE, vol. 11451 (2020): 114511P. Is in proceedings of: **SPIE Astronomical Telescopes + Instrumentation 2020**, Online Only, United States, 14-18 Dec 2020.

DOI: 10.1117/12.2560828

PROCEEDINGS OF SPIE

SPIEDigitalLibrary.org/conference-proceedings-of-spie

H2020 opticon project overview: Investigating the use of additive manufacturing for the design and build of multi-functional integrated astronomical components

Schnetler, Hermine, van de Vorst, Bart, Snell, Robert, Atkins, Carolyn, Miller, Chris, et al.

Hermine Schnetler, Bart van de Vorst, Robert M. Snell, Carolyn Atkins, Chris Miller, Katherine Morris, Szigfrid Farkas, György Mező, Mélanie Roulet, Emmanuel Hugot, Afrodisio Vega Moreno, Fabio Tenegi, Joris Dufils, "H2020 opticon project overview: Investigating the use of additive manufacturing for the design and build of multi-functional integrated astronomical components," Proc. SPIE 11451, Advances in Optical and Mechanical Technologies for Telescopes and Instrumentation IV, 114511P (13 December 2020); doi: 10.1117/12.2560828

SPIE.

Event: SPIE Astronomical Telescopes + Instrumentation, 2020, Online Only

H2020 Opticon WP5 Overview

Investigating the use of additive manufacturing (AM) for the design and build of multifunctional integrated astronomical components

Hermine Schnetler[a], Bart van de Vorst[b], Robert M. Snell[c], Carolyn Atkins[a], Chris Miller[a], Katherine Morris[a], Szigfrid Farkas[d], György Mező[d], Mélanie Roulet[e], Emmanuel Hugot[e], Afrodisio Vega Moreno[f], Fabio Tenegi[f], Joris Dufils[d]

[a]Science and Technology Facilities Council, UK Astronomy Technology Centre (United Kingdom) (United Kingdom), [b]TNO (Netherlands), [c]University of Sheffield (United Kingdom); [d]MTA Research Centre for Astronomy and Earth Sciences, Konkoly Observatory (Hungary), [e]Aix-Marseille University, CNES (France), Lab. d'Astrophysique de Marseille, CNRS (France), [f]Instituto de Astrofísica de Canarias (Spain)

ABSTRACT

Additive manufacturing (AM) methods and post processing techniques are promising methodologies considering that it is now possible to print in a wide variety of materials using processes much refined from those originally available twenty years ago. To date the uptake of AM in Astronomy is relatively low compared to other application areas, aviation being one such example. Due to the rapid progress made in additive manufacturing and the lack of its adoption in Astronomy, there are many opportunity to deploy new fabrication processes.

In this paper, we outline the project and report the results of our investigation to make use of additive manufacturing and novel materials in the fabrication of multi-functional integrated components fit for use in astronomy instrumentation, which can operate in cryogenic environments and space application.

Keywords: Additive manufacturing, 3-D printing, materials, processes, fabrication of reflective surfaces, and cryogenics

1. INTRODUCTION

Additive manufacturing (AM) methods and post processing techniques are promising methodologies considering that it is now possible to print in a wide variety of materials and many of the AM processes available today were invented more than twenty years ago. To date the uptake of AM in Astronomy is relatively low compared to other applications areas, most notably in aviation. Due to the rapid progress made in additive manufacturing and the lack of its adoption in Astronomy we need to catch-up with other application fields such as aviation and the manufacturing of engines.

Most astronomical instrument designs include reflective optical components such as mirrors. Intuitively one would assume that the first choice material for printing astronomical mirrors would be to select a metal and the associated printing technology. Based on the ASTM/ISO 52900:2015 standard there are seven (7) AM processes. The seven categories are extrusion, photopolymerization, powder bed fusion, material jetting, binder jetting, directed energy deposition, and lamination. Within the framework of the Horison2010 (H2020) Additive Astronomy Integrated-component Manufacturing (A2IM), first phase of the project the team has identified components where the use of AM will provide clear advantages and provides for compelling business cases. For each component, the required features and mechanical properties were defined and sample pieces were printed in a variety of materials using a number of processes to create a multi-dimensional matrix, which can be used to inform mirror designers.

Due to the layer-by-layer, build process directly from digital data AM provides the freedom to fabricate mirrors that is otherwise very difficult and expensive to make. Examples are active freeform, highly aspherical, and cooled mirrors. The uniqueness of the fabrication method also makes it possible to optimize the stiffness while also reducing the weight of the component.

Advances in Optical and Mechanical Technologies for Telescopes and Instrumentation IV,
edited by Ramón Navarro, Roland Geyl, Proc. of SPIE Vol. 11451, 114511P
© 2020 SPIE · CCC code: 0277-786X/20/$21 · doi: 10.1117/12.2560828

Current commercial optimization software is aimed at making rectangular and square components while typically in astronomy we favour round mirrors. The team has developed algorithms and modelling software specifically aimed to design optical components for 3D printing. Based on the results obtained the life-cycle processes for the fabrication of the following mirror types are reported in this paper; a CubeSat, Freeform, Active Mirror, and Cooled.

Normally ground-based (near- and mid-infrared) astronomical instruments operate in a cryogenic environment (vacuum and at cryogenic temperatures). Currently the materials used in the fabrication of components using additive manufacturing have not been fully characterized and evaluated in a cryogenic environment, thus very little information is available, and therefore it was an important component of this study.

2. PROJECT OVERVIEW AND SCHEDULE

The project kicked-off at the start of 2017 and we set out to investigate the use of additive manufacturing (also known as 3-D printing) for the fabrication of multi-functional astronomical components. A multifunctional component is a single component, which implements more than one function at a time. For example, an optical trombone can be used to redirect science light and it can compensate for path-length variations at the same time.

During 2017 and 2018, the team undertook a feasibility study. Firstly, the team prepared a list of frequently used astronomical components. For each component, the typical features and requirements have been identified. This was followed by the designing of a benchmark model that allowed us to define the limits for each of the most promising materials and 3-D printing processes. A detailed description of the benchmark model is given in Section 4 of this paper. Each benchmark part produced was visually inspected and the mechanical properties were measured where possible. On completion of the feasibility study, a study report was prepared. The report can be downloaded from https://www.astro-opticon.org/h2020/public-reports.html [1].

After the feasibility study, the team elected to focus on the integration of special features and mirrors that can be used in astronomical instruments such as imagers and spectrographs. The initial idea was to qualify these mirrors for cryogenic operations. Unfortunately, due to limited access to laboratories, the team has not managed to proceed as initially planned. We have received a no-cost extension until June 2021, however at this moment in time; nobody is sure, when things will return to normal.

Astronomical instruments are becoming ever larger and more complex as we seek to address the latest scientific questions. New techniques offer the potential to design and build components and thus instruments that are lighter, self-contained, and easier to assemble and align, resulting potentially in improved performance, more compact, reliable and possibly less expensive.

Our value statement can be summarized as follow: “Making use of additive manufacturing design, analysis and manufacturing processed to produce multi-functional integrated astronomical components with increased performance that are smaller, lighter, can be fabricated faster and therefore is more affordable, which is also kinder to the our planet over the life-cycle of the components and work efficiently in cryogenic environments.”

3. ADDITIVE MANUFACTURING PROCESSES

3.1 Introduction

As its name implies, additive manufacturing adds material to create an object. A more formal definition: “Additive manufacturing uses computer-aided-design (CAD) software to direct hardware to deposit material, layer upon layer, in precise geometric shapes.”

Due to the layer-by-layer, build process directly from digital data AM provides the freedom to fabricate mirrors that is otherwise very difficult and expensive to make. Examples of such mirrors are active freeform, highly aspherical, and cooled mirrors. The uniqueness of the fabrication method also makes it possible to optimize the stiffness while also reducing the weight of the component.

The advantages are numerous; here we list three main advantages:

1) Minimizing waste
2) Saving energy and time
3) Easily make non-geometric shapes as illustrated on this viewgraph.

In addition, because it is an all-digital workflow, we get rid of the so called "over-the-wall engineering". It forces multi-functional cooperation between the various engineering disciplines; it also promotes designers to become experience in a multitude of engineering skills, including designing for manufacturability.

Often it is very difficult for experience mechanical engineers to come to terms with the fact that they need to throw away traditional design experience, to allow them to learn a new approach to design for Additive Manufacturing. Although 3D printing is increasingly being utilised as a quick and efficient method for product prototyping, it requires a completely new way of thinking. Many organisations today will still develop two designs: (1) a 3D printed model to fabricate prototypes with and, (2) a design for producing manufacturing quantities, this is the case for most industries with the exception of the aerospace and car industries.

3.2 Pillars of additive manufacturing

The three pillars of additive manufacturing are based on: (1) the application defines the mechanical properties required; (2) the designer selects the material that could deliver the required mechanical properties. Based on the material the designer selects (3) a process that can fabricate the part in the selected material.

Table 1: Additive manufacturing three pillars.

APPLICATIONS	MATERIALS	MANUFACTURING PROCESSES
Space Mirrors	Stainless steel SS316	Powder-bed fusion
Cooled mirrors	Titanium Ti64	Selective Laser Sintering
Deformable mirrors	Aluminium	Selective Laser Melting
Freeform mirrors including active	Alumina	Binder Jetting
control elements such as:	PA12	VAT photopolymerization
Actuators	Bluestone	
Flexures		
Sensors		

Applications

The application area of interest is the design and manufacturing of integrated mirrors for ground and space astronomical instruments. The team focussed on the development of deformable, freeform active, CubeSat, and cooled mirrors.

To support the active mirrors the UK ATC also performed various studies to reduce the component count of the controllable actuation devices required in active and deformable mirrors. Here specifically a number of metal printing processes have been evaluated for the manufacturing of flexures. As part of the freeform active mirror experiment (FAME) it was found that it is almost impossible to bend the wire bond thin metal flexures into the same shape to exhibit the same repeatable mechanical characteristics. It was also found that working at millimetre scales it is very difficult to control the tolerance build-up when the part number count is in excess of five or more.

Materials

Materials for mirror fabrications have special requirements, therefor the material matters. The primary function of a mirror is to reflect light, without absorbing the photons, therefore the material must respond well to polishing. Materials that polish well are hard and dense. In addition, a low coefficient of thermal expansion (CTE) is a primary requirement to ensure stability, especially for space and cryogenic environment applications.

There are a wide range of materials available that can be selected for fabricated parts using additive manufacturing such as stainless steels, super alloys, titanium, cobalt, chrome, ceramics such as alumina and silicon carbide. Then there are also the various nylons as acrylonitile butadiene styrene (ABS), Polylactic acid (PLA), polyvinyl alcohol (PVA), and polycarbonate.

The materials investigate and used in the research of the work package five are listed in Table 1 above. This diversity of materials provides the ability to select the appropriate material for each application to provide the required stiffness, thermostability, transparency, or chemical resistance depending on the functionality required by the part. In addition, it is no longer necessary to trade between properties such as stiffness and reduced mass of a part.

Additive Manufacturing Processes

There are seven (7) AM categories in accordance with ASTM F2792/ISO 52900:2015. The seven categories are, vat photopolymerization, material jetting, binder jetting, material extrusion, sheet lamination, directed energy deposition, and powder bed fusion.

Vat photopolymerization uses a vat of liquid photopolymer resin, and the model is constructed layer-by-layer by using an ultraviolet light to cure or harden the resin where required. In material jetting, droplets of the build material are selectively deposited, while in binder jetting it is the liquid bonding agent that is selectively deposited onto the powder.

Selective laser melting (SLM) and selective laser sintering (SLS) are examples where focused thermal energy provided by sources, like lasers and electron beams, is used to melt the feedstock within a small area. This process is currently exclusively used for the fabrication of metal parts and falls under the category of powder bed fusion. Material extrusion (commonly known as FDM (fused deposition modelling)) on the other hand is a process in which heated material is selectively dispensed through a nozzle or orifice. Sheet lamination is a process in which sheets of material are bonded together to form an object. Sheet lamination includes ultrasonic additive manufacturing (UAM), and Laminated Additive Manufacturing (LOM).

Directed Energy Deposition (DED) is where material is deposited from a nozzle onto the surface of an existing object. Material is either in powder or wire form. The material is melted with using a laser, electron beam, or plasma arc upon the deposition, while powder bed fusion is where thermal energy selectively fuses regions of powder together. The thermal energy is obtain either by using a laser or an electron beam. Direct Metal Laser Sintering (DMLS), Selective Laser Melting (SLM), Electron Beam Melting (EBM), Selective Heat Sintering (SHS), and Selective Laser Sintering (SLS) are examples of Powder Bed Fusion techniques. Both DMLS and SLM produce parts in a similar way to selective Laser Sintering (SLS): a laser source selectively bonds together powder particles layer-by-layer. The main difference, of course, is that DMLS and SLM produce parts out of metal. The difference between the DMLS and SLM processes is subtle: SLM achieves a full melt of the powder particles, while DMLS heats the metal particles to a point that they fuse together on a molecular level instead.

Support structures are always required in DMLS and SLM to minimize the distortion caused by the high temperatures required to fuse the metal particles. After printing, the metal supports need to be removed either manually or through CNC machining. Machining can also be employed to improve the accuracy of critical features (e.g. holes). Finally, the parts are thermally treated to eliminate any residual stresses. Shown in Figure 1 are examples of DMLS and SLM fabricated metal parts.

Titanium Mirror (TNO/ESA)

Hydraulic Manifold (TNO Hydrauvision)

Titanium Acetabular hip cup (Adler Ortho)

Figure 1: Examples of Direct Metal Laser Sintering and Selective Laser Melting parts.

A high-power laser (in DMLS/SLM) or an electron beam (in EBM) is used to bond metal powder particles together selectively, layer-by-layer forming the metal part. In SLM and DMLS, almost all process parameters are set by the machine manufacturer. The layer height used in metal 3D printing varies between 20 to 50 microns and depends on the properties of the metal powder (flowability, particle size distribution, shape, etc.).

The typical build size of a metal 3D printing system is 250 x 150 x 150 mm, but larger machines are also available (up to 500 x 280 x 360 mm). The dimensionally accuracy that a metal 3D printer can achieve is approximately ± 0.1 mm.

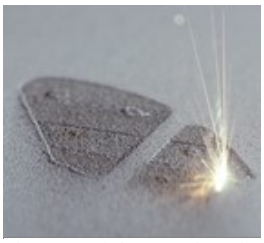

Figure 2: High power laser in DMLS and SLM.

The 3D printing step is only the beginning of the DMLS/SLM manufacturing process. After the print is complete, several (compulsory or optional) post-processing steps are required before the parts are ready to use. Compulsory post-processing steps include:

1) Stress relief; due to the very high processing temperatures during printing, internal stresses develop. These need to be relieved through a thermal cycle before any other operation.
2) Removal of the parts; in DMLS and SLM the parts are essentially welded onto the build platform. A band saw or EDM wire cutting is used here.
3) Removal of the support; support in DMLS/SLM is always required to mitigate the warping and distortion that occurs during printing. Support is removed manually or CNC machined.

Shown in Figure 3 is the design and manufacturing workflow to ensure an optimized design.

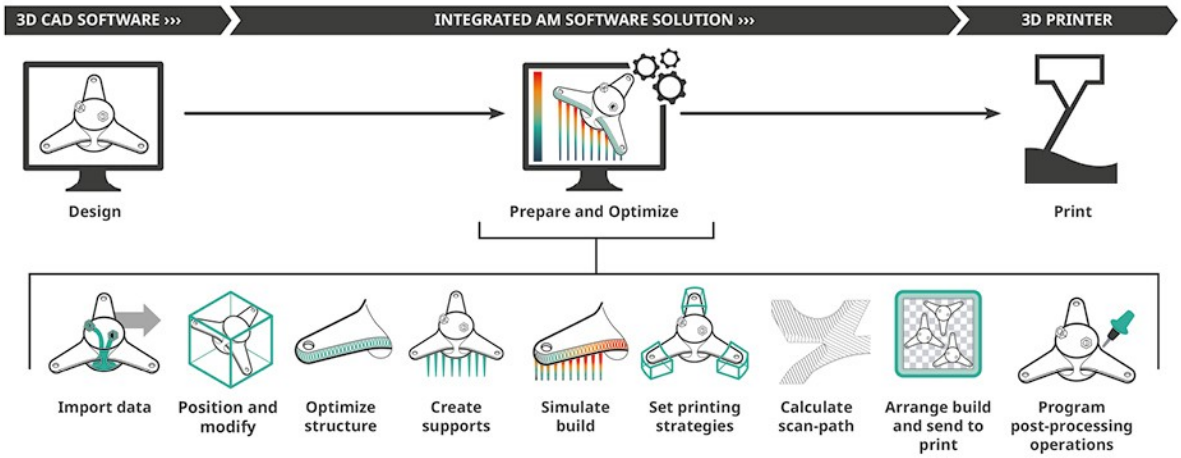

Figure 3: Additive process flow, which integrates the design and manufacturing process. During this process, it is very important for the design engineering to consult with the equipment operator and/or technician to ensure that the best results are achieved.

Within the framework of this project the team identified components where AM will provide clear advantages and provides for compelling business cases. The approach taken by the team was then to identify the materials they were interested to ensure that the integrated-component will comply with the mechanical and optical properties demanded by the chosen applications. Once the application requirements are defines and the material selected a printing technique and machine can be selected.

4. BENCHMARK MODEL

The team developed a benchmark including most of the typically features required in an integrated astronomical component. This benchmark model was fabricated in a variety of commercially available additive manufacturing materials. Once manufactured each model has been visually inspected under a microscope and where appropriate the mechanical properties have been measured. As part of the initial feasibility study test pieces have been manufactured and the mechanical properties have been measured. The feasibility report[1] can be downloaded from https://www.astro-opticon.org/h2020/public-reports.html.

4.1 Test geometry

Current AM standards working groups for the development of AM-related standards have been organized by the International Organization for Standardization (ISO/TC 261) and the American Society for Testing and Materials (ASTM F42). To date, they have produced standards related to terminology, individual processes, chains of processes (hardware and software), test procedures, quality parameters, customer-supplier agreements, and fundamental elements. Recent additions address data processing, consider the relevance of, and specify variations to existing standards. In 2013, ISO and ASTM defined a common goal to produce one set of global standards including general standards that are applicable to most AM materials, processes, and applications; category standards that define the requirements for a material or a process category; and specialized standards for specific requirements to a material, process or application. AM standardization efforts are also taking place in:

- Germany (VDI FA 105 and DIN NA 145-04-01AA),
- Spain(AEN/CTN 116),
- France (AFNOR UNM 920),
- Sweden (SIS/TK 563),
- US (SAE AMS-AM)
- UK (BSI AMT/8)

The Association of German Engineers published VDI 3404 and VDI 3405 as part of this work. AM standards provide a common understanding of the field and a shared lexicon from which to work. This is important for developing and using AM-related design tools and methodologies. It is also a prerequisite for developing design related AM standards. For example, ISO/ASTM DIS 20195 “Guide for Design for Additive Manufacturing” is currently under development.

4.2 Test artifacts

A new H2020 Opticon test geometry was designed to meet the requirements for lightweight and stiff optical components. Current available test artifacts from NIST and the DIN ISO ASTM 52902 standard inspired artifact from the University of Tirol were used as a guideline.

Table 2: Existing benchmark models, used as inspiration for the development of the H2020 Opticon benchmark model.

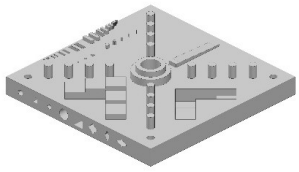	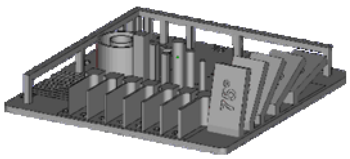	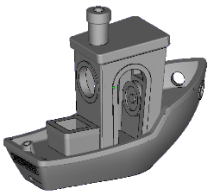
NIST artifact, designed by Shawn Moylan Available for download at NIST *www.nist.gov/topics/additive-manufacturing/resources/additive-manufacturing-test-artifact*	Artifact inspired by standard DIN EN ISO ASTM 52902 University of Tirol, Design by Markus Ehrlenbach Available for download at Thingiverse and GrabCad *www.thingiverse.com/thing:3511746*	3DBenchy Design by Creative Tools Available for download *www.3dBenchy.com*

Included in the H2020 Opticon benchmark model (image below) are:

- rectangular holes, bosses, and tubes,
- round holes, bosses, and tubes
- spherical holes and bosses,
- conical bosses,
- L-shaped bosses,
- ramps,
- overhangs,
- angles,
- side notches
- thin walls and fine features,
- freeform structures, and
- towers (higher aspect ratio than vertical bosses)

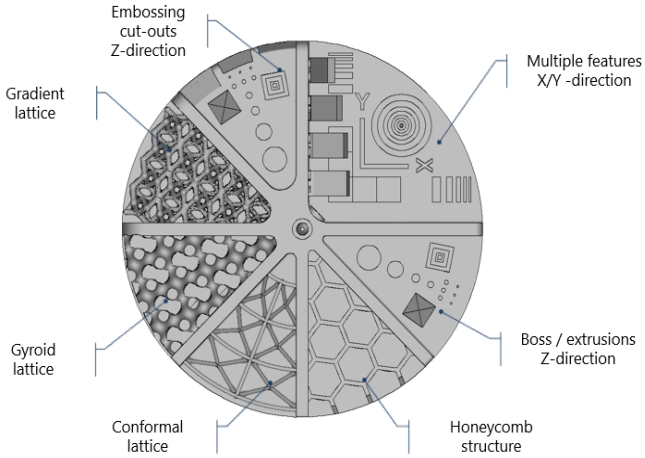

Figure 4: H2020 Opticon bench mark CAD model

The sizes of the test artefacts varied, but the largest observed dimension was of the square base of an artefact that was 240 mm by 240 mm. The smallest features observed were 0.25 mm thin walls (for both polymer-based and metal-based AM processes), 0.2 mm diameter holes and bosses in polymer-based AM processes, and 0.5 mm diameter holes and bosses in metal-based AM processes. The detail dimensions and geometries for the H2020 Opticon benchmark model are defined in Table 3 and Table 4. In Table 3 each feature is defined while in Table 4 the dimensions for the holes in one of the vertical walls are defined.

Table 3: Detailed characteristics definition for the multiple features included in the H2020 Opticon Benchmark model.

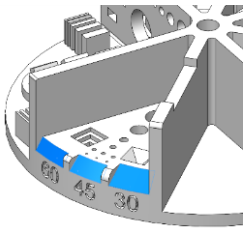	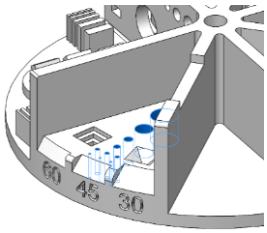	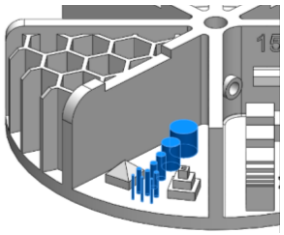
Chamfer 1.5 mm 30°, 45°, 60°	Vertical holes Depth: 3mm Ø 0.25, Ø 0.50, Ø 0.75, Ø 1.00 Ø 2.00, Ø 3.00	Vertical pillars Height: 3mm Ø 0.25, Ø 0.50, Ø 0.75, Ø 1.00 Ø 2.00, Ø 3.00
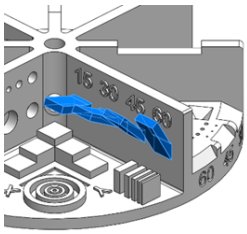	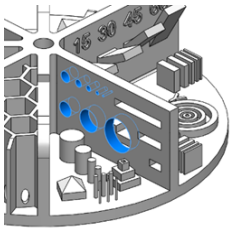	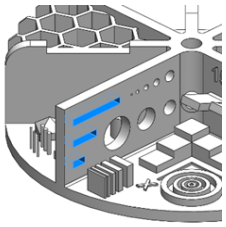
Angular overhang 3 x 4.5mm Angle: 15°, 30°, 45°, 60°	Horizontal holes Depth: 1.5 mm Ø 0.25, Ø 0.50, Ø 1.00, Ø 1.50	Horizontal overhang Depth: 1.5 mm Width: 2, 4, 8 mm

	Ø 2.00, Ø 3.00, Ø 4.50	
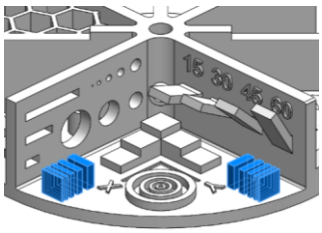	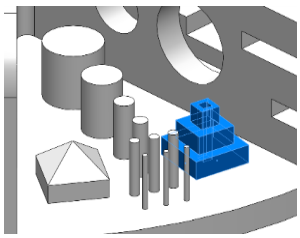	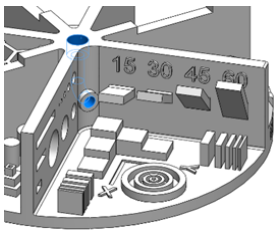
X & Y Wall thickness 3 x 3 mm Thickness: 0.23, 0.35, 0.5, 0.75, 1.00mm	Cube Pyramid Step size: 1mm Size: 3x3, 2x2, 1x1	Internal channel Diameter: Ø 1 mm

Table 4: Definition of the definitions of the dimensions for the vertical holes of the H2020 Opticon benchmark model.

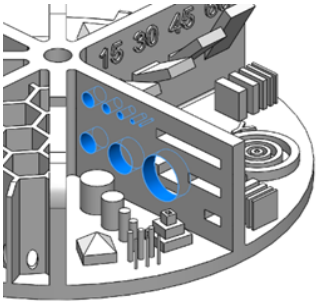

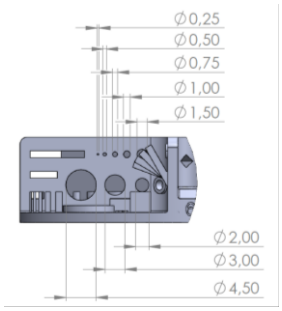

It is vitally important to consider any structures in your design that are freestanding. Things like cylinders, clips, walls and overhangs might need to be supported.

Thick or thin: in traditional manufacturing processes, thin materials can be reinforced by adding a range of fixings to mitigate potential weaknesses. However, as 3D printed designs are built in one continuous process with no added fixtures, thin walls and sections are vulnerable to collapse. When developing your 3D print design it is important to ensure that the walls are thick enough to ensure that the built is robust.

If the design incorporates holes and slots, these features create weaknesses in the built and can collapse if not designed correctly. Generally if the hole or slot is small (approximately less than 5 mm diameter) it can be printed without providing support. For larger holes, there is a range of options available. It is important to remember that while AM can be an option, not all parts required will be suitable.

Four benchmark models have been manufactured. These are depicted in Figure 5 below.

		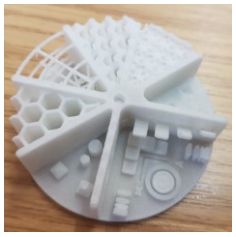	
TiAl6V4 Powder Bed Fusion	AlSi10Mg Powder Bed Fusion	Glass filled nylon SLS	PolyAmide 12 Multi-Jet Fusion

Figure 5: H2020 Opticon benchmark models printed in a variety of materials and using a number of additive manufacturing processes.

4.3 Powder bed fusion technologies and materials

There can be large differences between parts that are manufactured by Powder Bed Fusion. The initial build quality is determined by several factors. The main categories are part design, build orientation, material, process parameters, and the machine architecture. The build parameters are depending on the used material and the capabilities of the equipment. They are usually controlled by the equipment owner or service bureau.

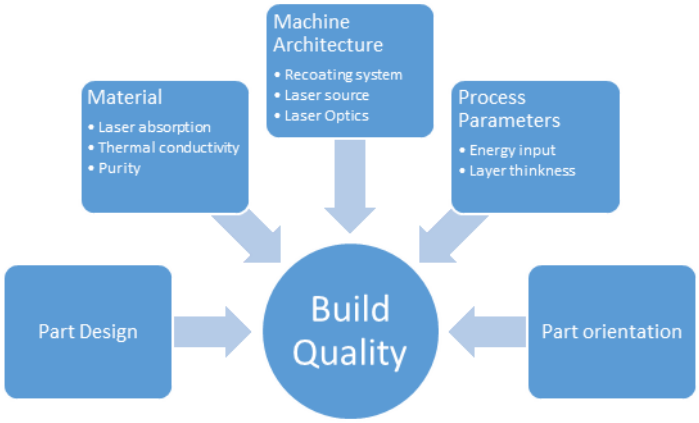

Figure 6: Build quality parameters.

Currently there are multiple manufactures of Powder Bed Fusion systems. All with their specific machines and processes. Machines are developed with different applications and needs in mind. From small-scale machines for high-resolution parts too large high-performance system for series production.

Table 5: Powder Bed Fusion systems and equipment specifications.

Machine	MLab - R	SLM 500HL
		
Manufacture	ConceptLaser by GE	SLM Solutions
Build volume (XYZ)	90 x 90 x 80 mm	500 x 280 x 365 mm
Layer Thickness	15 – 30 µm	20 – 200 µm
Laser system	100W	Twin 2x 400W
		Quad 4x 400W
Beam Focus Diameter	50 µm	80 – 120 µm
Maximum Scan Speed	7 m/s	10 m/s
Build rate	1 – 5 cm^3/h	up to 170 cm^3/h
Cost	>175 K Euro	>1M EURO

Difference in materials

There is also a large difference in processability of materials. There are materials with low reflectivity and low thermal conductivity such as titanium, ferrous, and nickel alloys, and materials with high reflectivity and high thermal conductivity such as aluminium and copper alloys.

The later are more difficult to process due to the low absorptivity of laser energy and the high coefficient of thermal expansion. In addition, the latent heat of fusion for aluminium (the energy required for melting) is the highest for any metal. Therefore, applying sufficient energy in the laser-powder bed interaction zone and keeping that energy within the melting zone is very challenging. Controlling the melt pool and to achieve thin wall thicknesses and small features is difficult. The reactiveness and presence of oxides and hydrogen makes Aluminium even more susceptible to porosity and micro crack formation.

The preliminary visual inspection results of the special features for the H2020 Opticon benchmark model printed in TiAl6V4 and AlSi10Mg are summarized in Table 6.

Table 6: H2020 Opticon benchmark model printed in TiAl6V4 and AlSi10Mg visual evaluation summary.

TiAl6V4	AlSi10Mg
	
Well defined features and edges. Limited amount of sagging. Better surface quality	*Features are missing and edges are rounded the surface texture is rough, while the overhanging structures are sagging Rough surface texture*
	
Ø 0.25 mm holes are present and well defined. Debossed text is clearly readable.	*Ø 0.5 mm holes are present Debossed text is unclear.*
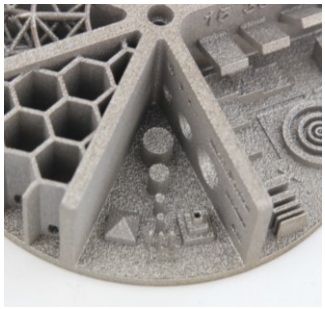	
Ø 0.25 mm pillars are present. Vertical walls are well defined.	*Ø 0.5 mm pillars are present. Veritcal walls are present but not well defined.*

Detail visual inspection observations regarding the special features for four models printed in different materials and using different AM processes are summarized in the Tables below. It is important to note that all the results shared in Tables 7 to 17 are preliminary results, and the author warn the readers not to jump to any premature conclusions based on the results presented here. The final report is due in the summer of 20201, where the quantitative data gathered will be published as part of this study.

Table 7 Visual inspection notes for AlSi10Mg. From the images, one can see that the small holes display no clear definition and there is some sagging, while the larger holes is tear shaped.

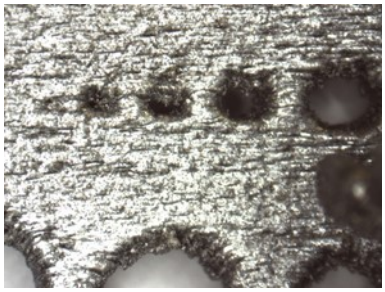
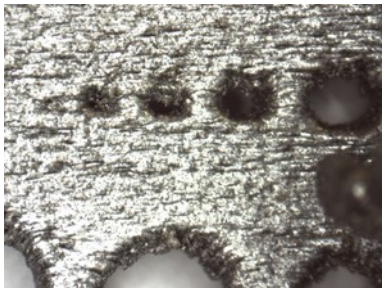
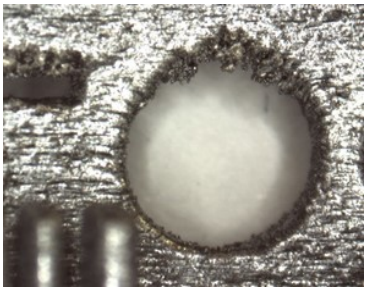

Ø 0.25	Ø 0.50	Ø 0.75	Ø 1.00	Ø 1.50	Ø 2.00
not present	blocked	open	open	open	open
		0.3 mm	0.6 mm	1.1 mm	1.5 „

Table 8: Visual inspection notes for TiAl6V4 build utilizing powder bed fusion. From the images one can see that the small holes are oval shaped, while the larger holes are sagging.

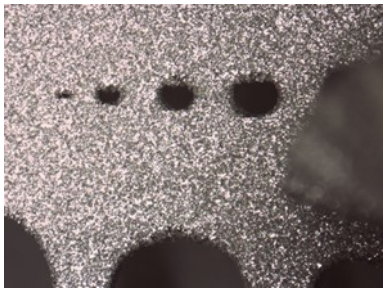
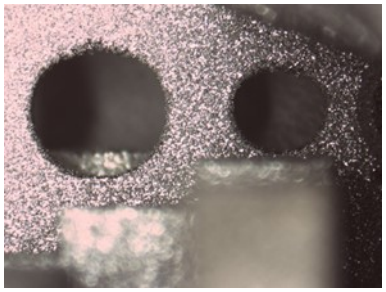
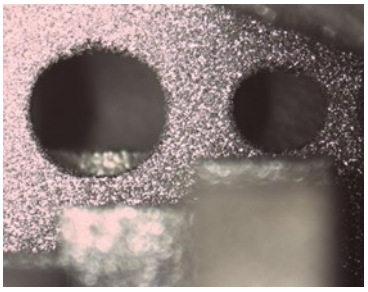

Ø 0.25	Ø 0.50	Ø 0.75	Ø 1.0	Ø 1.50	Ø 2.00
present	open	open	open	Open	Open
blocked	0.3 mm	0.60 mm	0.8 mm	1.3 mm	1.8 mm

Table 9: Visual inspection notes for PolyAmide PA12 printed with a powder bed fusion 3D printer. From the images one can see that the small holes display clear and there is no evidence of sagging. Horizontal ceiling defined clearly by the layer thickness.

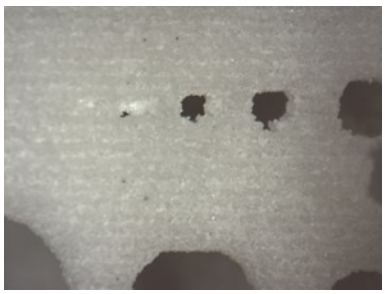
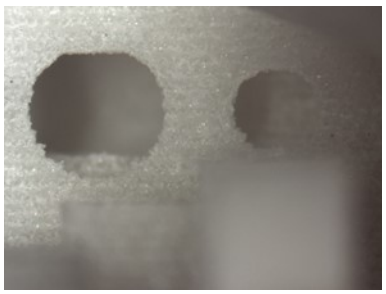
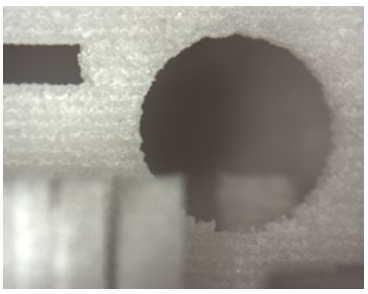

Ø 0.25	Ø 0.50	Ø 0.75	Ø 1.00	Ø 1.50	Ø 2.00
not present	open	open	Open	Open	Open
	0.25 mm	0.5 mm	0.8 mm	1.2 mm	1.5 mm

Table 10: Visual inspection notes for H2020 Opticon benchmark model printed in VisiJet with stereolithography. From the images, one can see that the small holes are clear and there is no evidence of sagging. You can clearly see the support structure in place for the 1.5 mm and 2.0 mm holes.

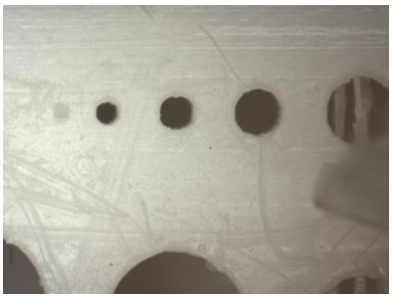
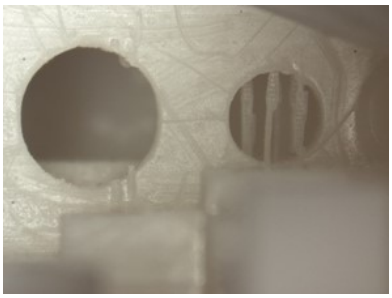
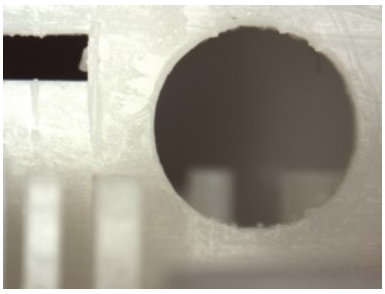

Ø 0.25	Ø 0.50	Ø 0.75	Ø 1.00	Ø 1.50	Ø 2.00
blocked	open	open	open	blocked	blocked
	0.5 mm	0.7 mm	1.0 mm	support	support
				1.5 mm	2.0 mm

Table 11: Visual inspection notes for H2020 Opticon benchmark model printed in Objet Vero Clear using material jetting. The small hole is blocked while the larger holes have clear definition. Some soluble support residue are left behind. There are also clear support marks visible on the vertical walls.

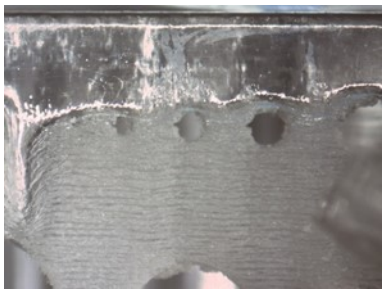
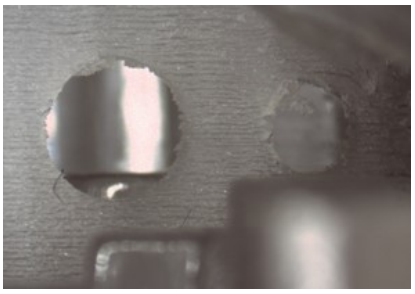
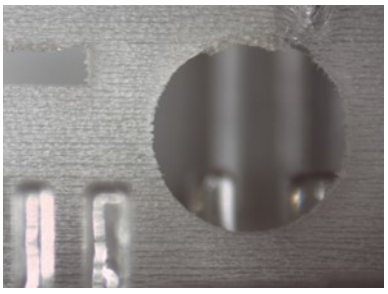

Ø 0.25	Ø 0.50	Ø 0.75	Ø 1.00	Ø 1.50	Ø 2.00
not present	Open	open	open	open	open
	0.36 mm	0.6 mm	0.86 mm	1.2 mm	1.8 mm

Angular overhang

Shown Figure 7 are the design details and a summary assessment of the quality of the angular overhangs for the four printed benchmarks. The angular overhangs where printed unsupported and the area of each overhang is 3.0 x 4.5 mm.

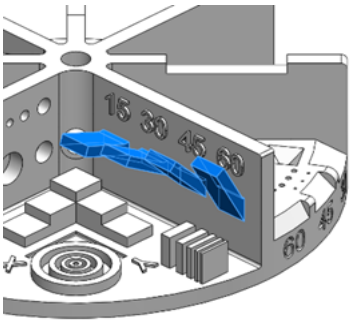

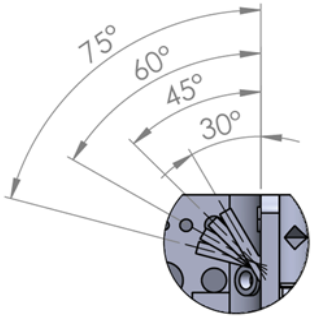

Figure 7: Overhang design and specifications.

Table 12: Powder Bed Fusion – AlSi10Mg: down facing surface s are sagging and the surfaces are rough. The quality is decreasing for the larger overhanging angle.

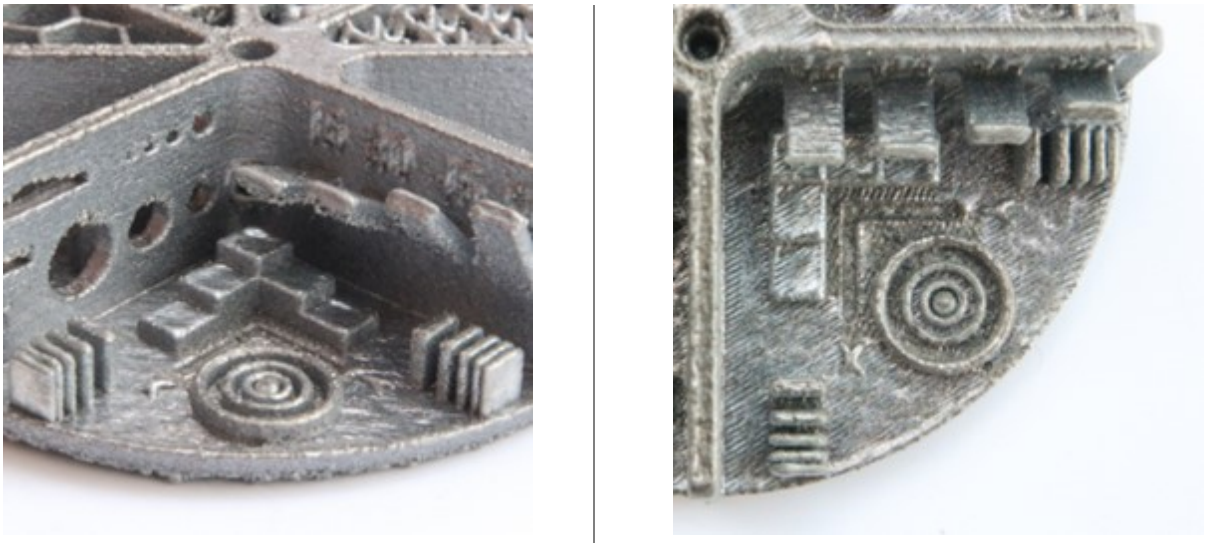

60° and 30°	45° and 45°	30° and 60°	15° and 75°
good surface quality			Poor surface quality

Table 13: Powder Bed Fusion – TiAl6V4: the down facing surface quality is good. Large overhanging surface are sagging and the surfaces are rougher.

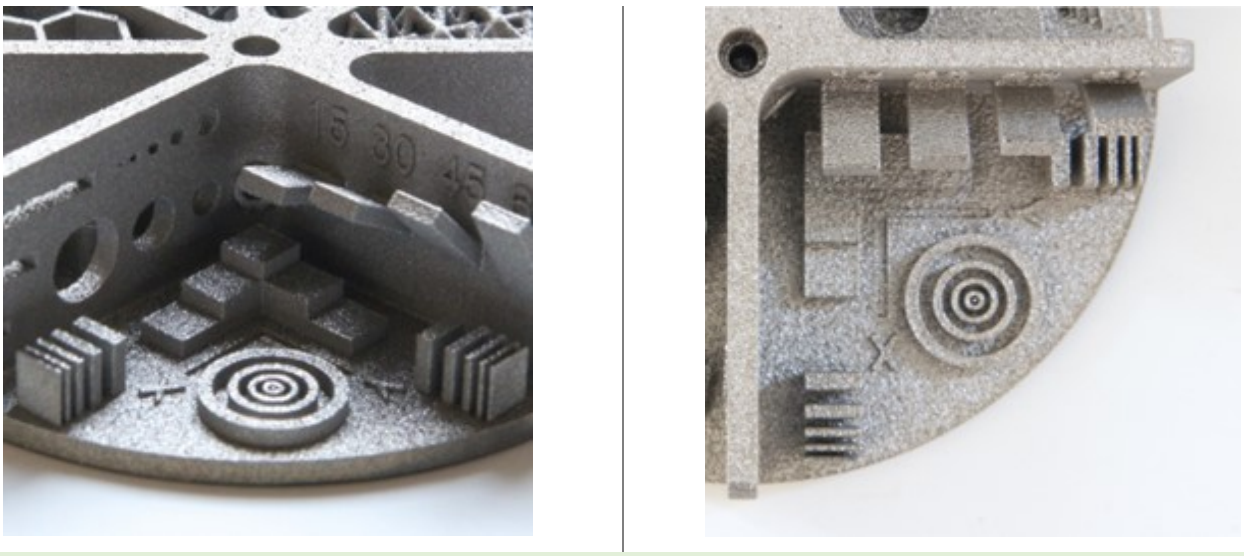

60° and 30°	45° and 45°	30° and 60°	15° and 75°
good surface quality	good surface quality	good surface quality	good surface quality

Four lattice structures were included in the H2020 Opticon bench model, namely: hexagon honeycomb, conformal, gradient, and gyroid. The results for each model printed are summarized below.

Hexagonal honeycomb grid structure

Honeycomb sandwich structures are designed to have a high stiffness-to-mass where the stiff, strong face sheets carry the bending loads, while the core resists shear loads. Model design and results are shown and summarized in Table 14.

Table 14: Honeycomb structure and visual print results.

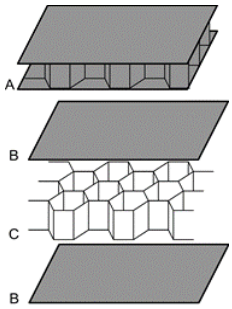

Diagram of an assembled composite sandwich (A), its constituent face sheets or skins (B) and honeycomb core (C)

https://en.wikipedia.org/wiki/Sandwich-structured_composite

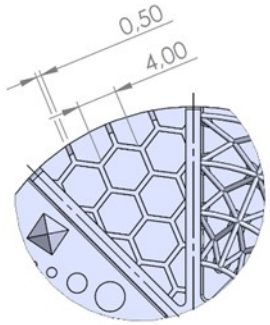

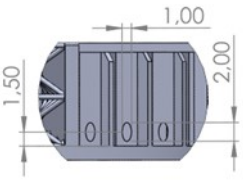

For easy residual material removal, multiple oval holes are incorporated in the design at the bottom of de cavity.

PBF AlSi10Mg	PBF TiAl6V4	PBF PA12	Stereolithography VisiJet
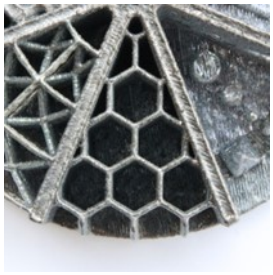	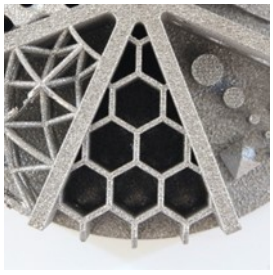	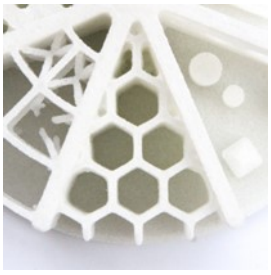	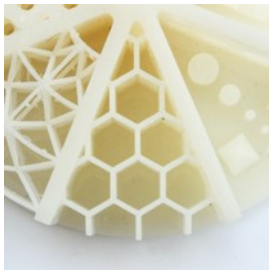
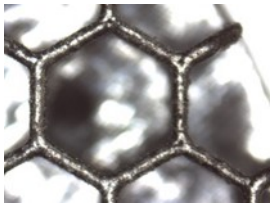	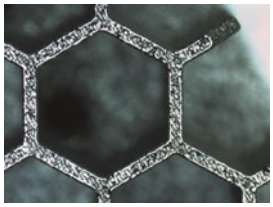	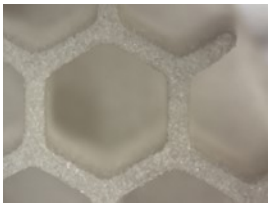	
Wall thickness: 0.51mm Side to side: 3.95mm	Wall thickness: 0.51mm Side to side: 4.0 mm	Wall thickness: 0.65mm Side to side: 3.85mm	Wall thickness: 0.48mm Side to side: 4.13mm
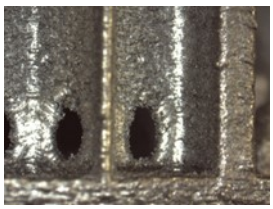	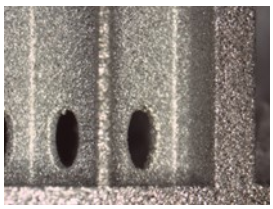	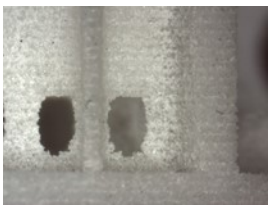	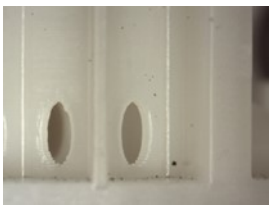
Downfacing surface display sagging Height: 1.55 mm Width: 0.83 mm	Oval holes display clear definition Height: 1.55 mm Width: 0.83 mm	More round than oval Height: 1.9 mm Width: 1.2mm	Very clear and crisp definition Height: 1.55 mm Width: 0.83 mm

Conformal lattice

Conformal lattice: CAD software is used to design a conformal lattice structure with a combination of a Primitive Cubic (cP) and a Body-Centered (BCC) cubic unit cell. The structure is build-up with Ø0.5 mm diameter struts in various directions and angles as illustrated below. The results for the four-benchmark models are summarized below.

Table 15: Conformal lattice design and visual results.

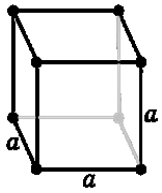	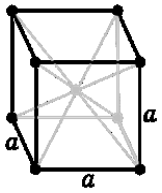	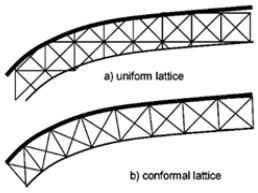	
Primitive Cubic consists of one lattice point on each corner of the cub	*Body Centered Cubic has one lattice point in the center of the unit cell in addition to the eight corner points.*	*The unit cells are conformal to the surface. A unit size of*	*Round struts with a diameter of 0.5 mm.*
PBF AlSi10Mg	PBF TiAl6V4	PBF PA12	SLA VisiJet
	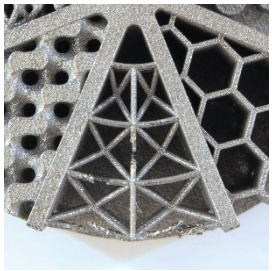	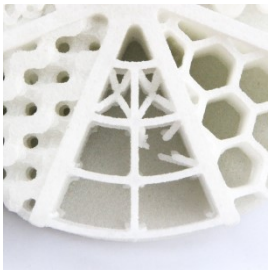	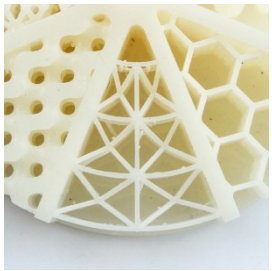
Defect free. All struts present	*Defects on horizontal struts. Some missing*	*Defects on angular struts* *Multiple struts missing*	*Defect free. All struts present*
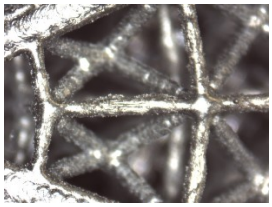	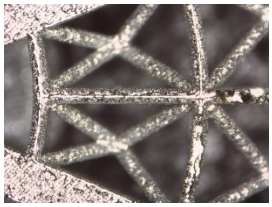		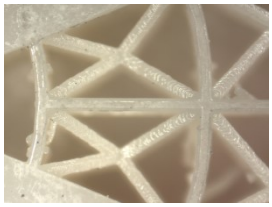
Strut stickness *Cp: 0.5 – 0.9 mm* *BCC: 0.7 – 0.9 mm*	*Strut stickness* *Cp: 0.5 mm* *BCC: 0.5 – 0.65 mm*	*Strut stickness* *Cp: 0.69mm* *BCC: 0.64 mm*	*Strut stickness* *Cp: 0.44 mm* *BCC: 0.49 mm*
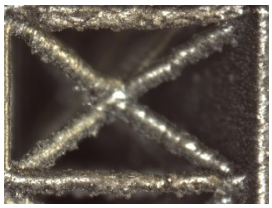	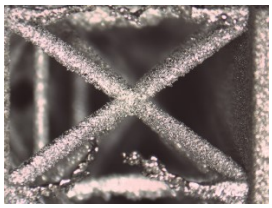		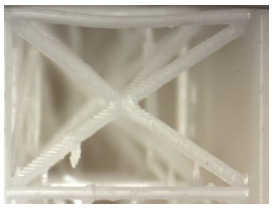
All struts are present. Down facing surfaces display sagging and	*Horizontal struts with large overhang are missing or display poor quality*	*Multiple angled struts are missing. Horizontal struts are present*	*All struts are present and of good quality. Some support structures present.*

Gradient lattice structure

With several 3D software packages, it is possible to automatically generate and edit complex lattice structures. Autodesk Netfabb Premium software is used to create a conformal volume lattice structure based upon a 3D STL file of the pie-shape. Summarized below are the gradient lattice structure results of the four-benchmark models evaluation the gradient lattice structure.

Table 16: Gradient lattice design and visual inspection results.

		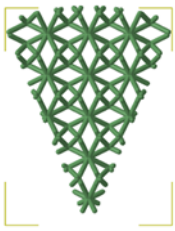	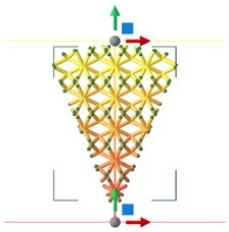	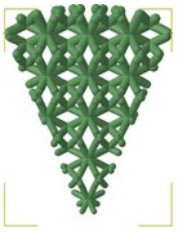
	3D STL file of the requested volume	*Isosahedron volume lattice structure* *3.5 x 3.5 x 3.5 mm*	*Determine gradient position and dimensions*	*Volume lattice with 0.5 to 1 mm gradient*
	PBF AlSi10Mg	PBF TiAl6V4	PBF PA12	SLA VisiJet
Gradient Lattice			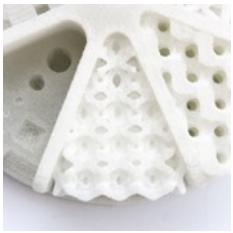	
	Defect free. All struts present	*Defect free. All struts present*	*Defect free. All struts present*	*Defect free. All struts present*
Top view XY		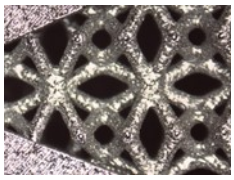	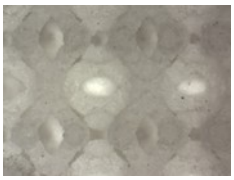	
	Rough surface in corners	*Clear definition*	*Clear definition. Residual powder present*	*Clear definition*
Side view XZ		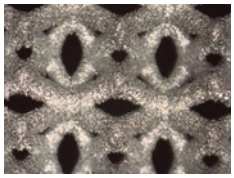	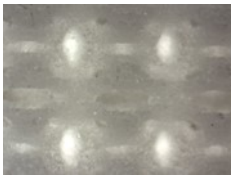	
	Sagging present on down facing surfaces. Holes partly blocked	*Some sagging on down facing surfaces. Holes are open*	*Cavities are blocked by residual powder*	*Clear definition. Support structure is present and can't be removed*

Gyroid lattice structure

The gyroid is the only known embedded triply periodic minimal surface that possesses triple junctions and no lines of reflectional symmetry. A gyroid surface can be trigonometrically approximated by a short equation:

$$\sin x \cos y + \sin y \cos z + \sin z \cos x = 0$$

The gyroid structure is this example is designed with Gen3D software. The gyroid structure in this example was designed with GEN3D software.

Table 17: Gyroid lattice summary of visual inspection results.

PBF AlSi10Mg	PBF TiAl6V4	PBF PA12	SLA VisiJet
	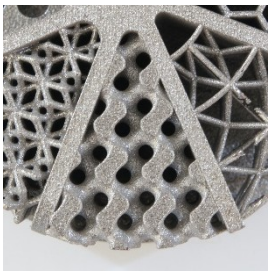	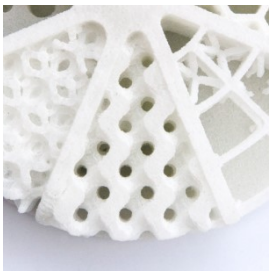	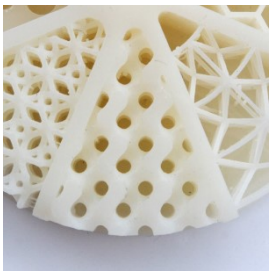
	Clear definition of structure		*Clear shape definition*
	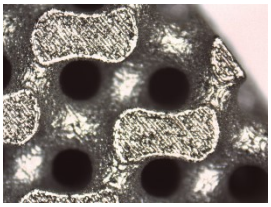		
Clear shape definition *Some splatter*	*Clear shape definition*	*Clear definition but some redidual powder*	*Clear shape definition*
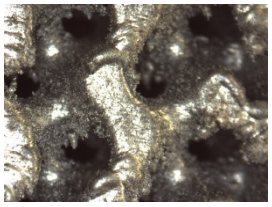	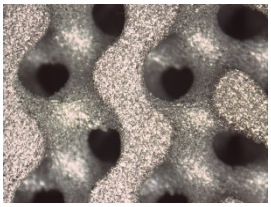	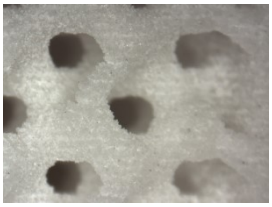	
Down facing surfaces		*Oval shape holes due to Z-bonus. Some residual powder*	*Non-removed support structure*

5. PROTOTYPING ASTRONOMY INTEGRATED MIRRORS

Telescopes are characterized by the collecting efficiency defined by the area of the primary mirror and the spatial resolution defined by λ/D, where D is the diameter of the primary mirror. Therefore in the advances of astronomy, observers constantly want to see further back in time (hence the request for a larger photon bucket) and to observe astronomical components in finer and finer detail (hence the requirement for the ever increasing diameter of the primary mirrors. To collect an increasing number of photons, development on large primary mirrors are undertaken, both ground-based and space-born telescopes increased their aperture. Segmented primary mirror technology allowed the increase of the diameter, firstly implemented on ground-based telescope this technique is now transposed to space telescopes. Observations covering the whole electromagnetic spectrum allow observers to study a wide variety of astronomical objects. This study set out to cover the whole electromagnetic spectrum as illustrated in Figure 8.

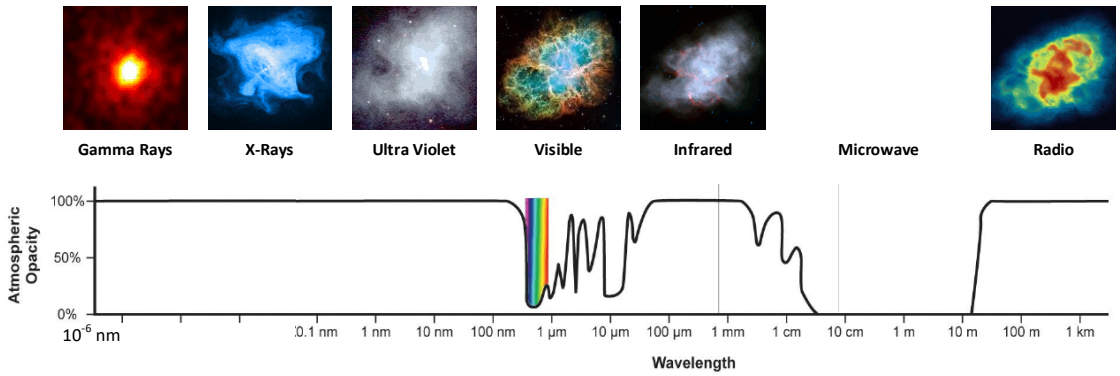

Figure 8: Electromagnetic spectrum showing the Crab Nebula observed at the different wavelengths from gamma rays to Radio frequencies.

Optical mirror surface characteristics are defined by the surface figure and roughness. The deviation from the ideal mirror is defined as the Surface Form Error (SFE). Three SFE domains are defined namely:

1) Low Spatial Frequency (LoF).
2) Mid Spatial Frequency (MiF).
3) High Spatial Frequency (HiF).

Based on the optical design and the wavelength the limits of these frequency domains vary a lot. The geometrical surface figure of a mirror (z) can be describe by the conic equation:

$$z = \frac{r^2}{R_c + \sqrt{R_c^2 - (1+K)r^2}}$$

K is the conic constant, R_c the radius of curvature, and r the diameter. The shape of the mirror will be a sphere for $K = 0$, and a parabola for $K = -1$.

Shape	Conic constant value
Hyperbolic	$K < -1$
Parabolic	$K = -1$
Elliptic elongated	$-1 < K < 0$
Spherical	$K = 0$
Elliptical	$K > 0$

The geometrical definition of the surface figure only describes the on-axis symmetrical surfaces. An alternative approach is to use a surface map instead of a surface figure. This allows the designer to include the off-axis portions of mirror, adding more optimization degrees of freedom as illustrated in Figure 9.

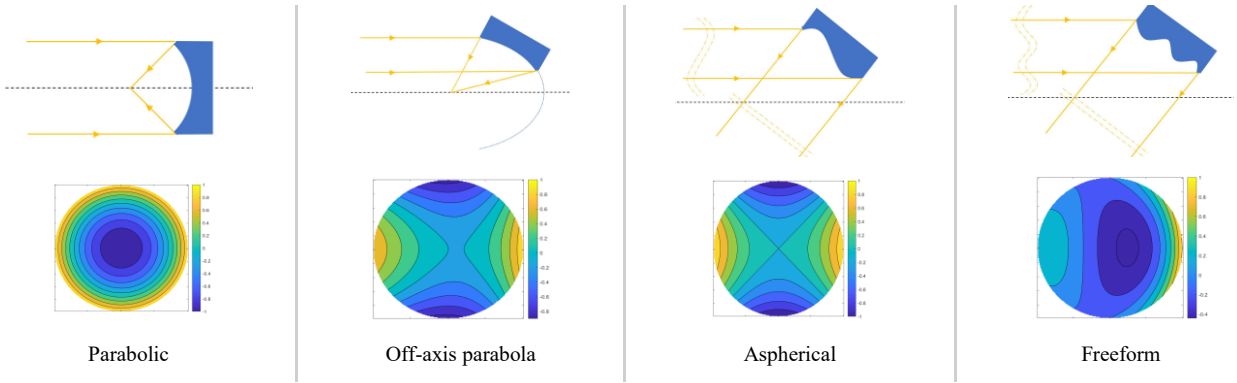

Figure 9: Surface maps for a parabolic, off-axis parabola, aspherical, and freeform mirrors. Credit: Roulet [2]

5.1 Deformable mirrors

In the field of space instrumentation, the challenge is to optimise the size and weight of optical components and not compromising on the optical performance such as surface quality and surface form. In the context of deformable and freeform mirrors, 3-D printing provides technical solutions to eliminate unnecessary interface chains by printing the mirror, the active array, and the support structure in one-step. Deformable mirrors (DM) are often made in ceramic, using traditional manufacturing methods; as such, 3D printing is the logical step for this investigation. A proof-of-concept study was performed, to test the feasibility of 3D printed Deformable Mirrors. This part of the project was led by the Laboratoire d'Astrophysique de Marseille (LAM). The work focussed on whether "print-through" can be eliminated by printing the active array structure directly on the back of a flat mirror.

Therefore, a mirror with an integrated radial rib structure has been designed and printed to investigate what the impact of the active array and support structure printed on the back might have on the surface quality of the mirror side of the part after polishing. To stiffen up the mirror face to obtain better results during the polishing, two designs were made (see Figure 10). Four samples of each design (circular and honeycomb) were made in alumina, and titanium (Ti64). A second set of Ti64 mirrors were made and subjected to a process known as hot isostatic pressing (HIP). HIP is a process in which components are subjected simultaneously to heat and high pressure in an inert gas to eliminate pores and remove defects. Sample mirrors of have been printed and some of these are depicted in Figure 11. The alumina-manufactured mirrors were polished and good results have been obtained.

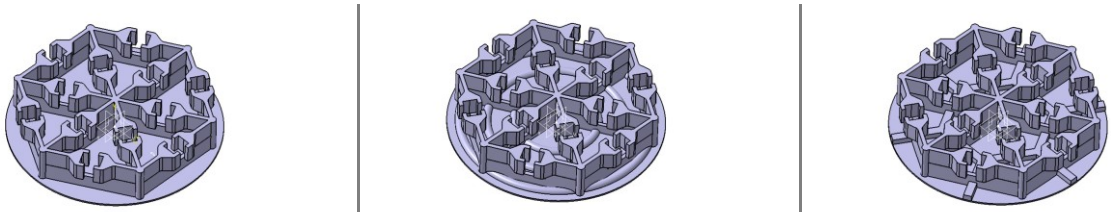

Radial active structure without extra support | With added material in concentric rings | With added material in the shape of a honeycomb

Figure 10: Deformable mirror designs with integrated active structure printed on the back of the mirror.

Alumina mirror side | Alumina back of mirror | Alumina (1.0 mm) after polishing

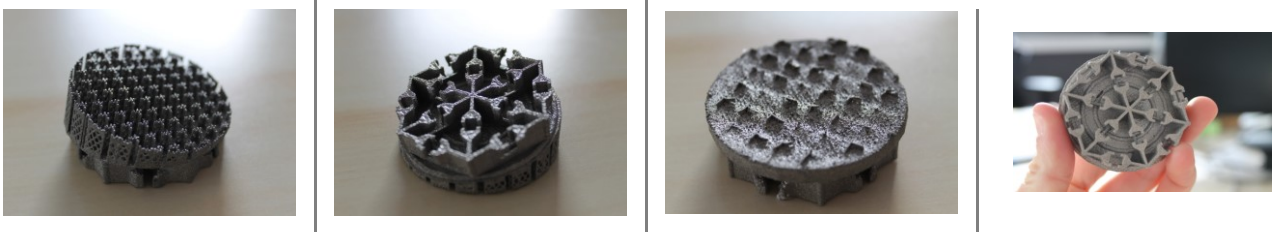

Ti64 3 mm thickness on the Arcam Q20+ (electron beam)

Figure 11: Deformable mirrors with integrated active array and support structure at the back of the mirror prototypes produced in Alumina and Titanium.

It should be very interesting to compare the results of this experiment with that of the Freeform Active Mirror Element (FAME). Unfortunately, the glueing of the feet onto the back of the hydro-formed highly aspherical mirror face introduced deformation on the front face of the FAME mirror.

5.2 Freeform active mirrors with integrated active arrays

In conjunction with WP4, we investigated the use of AM for the design and manufacturing of a Freeform Active Mirror to replace the traditional fabrication methods. While characterising the performance of the freeform active mirror element it was clear that the complexity of the product was very sensitive to the variation in the mechanical component tolerances. Therefore, the mirror was an excellent candidate to be produced with additive manufacturing.

Figure 12: Freeform active mirror printed in PA12

For this work, it was decided to use regenerative design methods. A prototype in PA12 using a material jetting process was fabricated and is depicted on the left (Figure 12). There are countless ways to determine print orientations. One consideration would be to reduce the post-processing steps.

To support the active mirrors the UK ATC also performed various studies to reduce the component count of the controllable actuation devices required in active and deformable mirrors. Here specifically a number of metal printing processes have been evaluated for the manufacturing of flexures. As part of the freeform active mirror experiment (FAME) it was found that it is almost impossible to bend the wire bond thin metal flexures into the same shape to exhibit the same repeatable mechanical characteristics. It was also found that working at millimetre scales it is very difficult to control the tolerance build-up when the part number count is in excess of five or more. This work is detailed by Farkas [3] et al (2020).

5.3 CubeSat mirror development

In the field of space instrumentation, the challenge is to optimize the size and weight of optical components and not compromising on the optical performance such as surface quality. Developed a mirror fabrication process for space applications. The objective of this development was to develop a process chain in the development of a lightweight AM metal mirror for integration within a CubeSat chassis. The mirror should highlight the unique aspects of additive manufacture as a fabrication process by demonstrating part consolidation and lightweight lattices. In the field of space instrumentation, the challenge is to optimize the size and weight of optical components and not compromising on the optical performance such as surface quality.

The design process and incorporation of the relevant modifications to ensure that the final design meets the CubeSat specification and the fabrication constraints required a six months design iteration phase followed by a shorter manufacturing and evaluation phase.

Started with four concept designs these were iterated upon by University of Sheffield and RAL Space Precision Development Facility (PDF) to create a design that exhibited a conformal lattice with both the mirror and mount geometry and a design that could have an optical surface generated via single point diamond turning (SPDT).

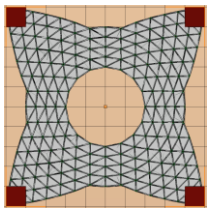

Figure 13: CubeSat lattice design

A highlight of this development was the development of a mirror specific lattice generation algorithm for the optimization of “sandwich mirrors”, where two parallel surfaces are supported by a filling lattice, a family of structures that offer excellent mechanical property to weight ratios. However, these lattices are based on unit cells that are cuboidal or prismatic and so do not have perfect fit with the typical mirror geometry. Edges of the mirror are left unsupported and curved mirrors result in incomplete unit cells. These problems were highlighted by Atkins et. al.[4] in previous SPIE presentations.

This novel lattice-generation-algorithm is formed by the use of interconnected concentric circles, which provides a symmetric and uniform level of support underneath the surface of the mirror. Controlling the location of every node allows heights to be adjust and curved mirrors to be supported precisely. This work is detailed by Snell et.al.[5] in paper 11451-6 of this conference.

6. ADDITIVE MANUFACTURING COOKBOOK

The Additive Astronomy Integrated Component Manufacturing workflow can be depicted by the three rings, which are used to also present the three AM, pillars. Firstly, you will need to perform a functional analysis, to define and specify what the part should do. Thereafter you should select a material that will provide you with the required mechanical and optical properties. Based on the preferred material, an AM process can be selected.

If more than, one process is suitable you might want to either perform a trade-off study or print multiple prototypes for evaluation. It is always a good idea to prepare an AM business case. Once the material and the printing method have been selected, the build can be planned.

While developing the idea of designing mirrors that have cooling channels embedded in the supporting structure, the team at the Instituto de Astrofísica de Canarias in Spain realized that the time it takes using the standard finite element analysis tool during optimization is very time consuming. In order to mitigate this problem, IAC has developed a modelling method, called "Continuum Material Equivalent". In this method, cellular material is treated as a continuous mass. This method is described in detail by Vega [6] et.al in paper 11450-84 of this conference.

One of the primary deliverables of this A2IM H2020 Opticon work package is to prepare, and make available to the astronomy community, an additive manufacturing cookbook. This cookbook will be made available in a similar manner as the feasibility study report, and should be available in the summer of 2021.

7. VISION

When additive manufacturing is used for the right reasons, it surely can be a massive game changer. My vision is to 3D print a complete fiber pick-off unit, such as the ones currently being built, and that will be used in the Very Large Telescope (VLT) Multi-Object Optical and Near-Infrared Spectrograph. Depicted on the right is an artist impression of a cluster of fiber pick-off units. Personally, I do not think this option is far away, as soon as multi-material 3D printers are becoming more readily available, my concept (patent pending) can be realized. By printing the mechanical structure around the optical fiber, the fiber micro-lens, the two rotational arms, the driver, and the driving electronics on a single AM machine in one go.

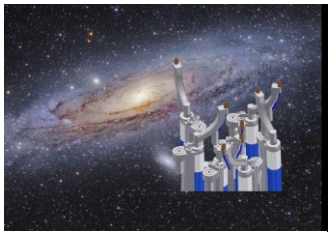

Figure 14: Vision of printing Fiber Pick-Off Unit (FPU) clusters

A final thought: It is not the intention that AM should replaces all of the current widely used traditional manufacturing techniques. It is just another useful method, which have its advantages and disadvantages, like anything else in the world. There is no silver bullet.

ACKNOWLEDGEMENTS

This project has received funding from the European Union's Horizon 2020 research and innovation programme under grant agreement No 730890. This material reflects only the authors' views and the Commission is not liable for any use that may be made of the information contained therein.

The author would also like to thank the team for their hard work and dedication to the project from all the participating research institutions.

REFERENCES

[1] Snell, R., et.al., "Report on Additive Manufacturing Materials for Opticon Work Package 5.1.1", 2019, https://www.astro-opticon.org/h2020/public-reports.html.
[2] Roulet, M., "3D printing for astronomical mirrors", Aix-Marseille Université, (2020).
[3] Farkas, S., Schnetler, H., van de Vorst, B., Rodenhuis, M., et. al., "Freeform active mirror designed for additive manufacturing", SPIE (2020).
[4] Atkins, C., Brzozowski, W., Dobson, N., Milanova, M., Todd, S., Pearson, D., Bourgenot, C., Brooks, D., Snell, R., Sun, W., Cooper, P., Alcock, S. G., and Nistea, I.-T., "Additively manufactured mirrors for CubeSats," Proc. SPIE 11116, Astronomical Optics: Design, Manufacture, and Test of Space and Ground Systems II, 1111616 (16 September 2019).
[5] Snell, R.M., Todd, I., Hernandez-Nava, E., Atkins, C., Schnetler, H., et. al., "An additive manufactured CubeSat mirror incorporating a novel circular lattice", SPIE (2020).
[6] Vega, A., Tenegi, F., Márquez, J.F., Schnetler, H., Atkins, C., Miller, C., Morris, K., Snell, R., van de Vorst, B., Dufils, J., Brouwers, L., Roulete, M., Hugo, E., Farkas, S., Mezo, G., "Design for Additive Manufacture (DfAM): The "Equivalent Continuum Material" for cellular structures analysis", SPIE (2020).